Journal of International Scientific Publication:
Materials, Methods & Technologies, Volume 3

BASIC MECHANICAL PROPERTIES OF PASTE FACADE RENDER MIXES WHEN INCORPORATING PHOTOCATALYTIC TITANIUM DIOXIDE

Jan Přikryl[1], Tomáš Melichar[1],

[1] Brno University of Technology, Faculty of Civil Engineering,

Institute of bulilding materials and Components Technology, Veveří 331/95,

602 00 Brno, Czech Republic

E-mail: prikryl.j@fce.vutbr.cz, melichar.t@fce.vutbr.cz

Abstract

Paste facade renders are produced mainly to supply new activity within the building industry or the increasing trend of applying exterior thermal insulation to pre-constructed domestic houses and flats. These facade renders are supplied in a soft paste form, dispersed with differing binding agents, such as acrylate, silicon, or silicate. White titanium dioxide (TiO_2), in the crystalline form of surface treated rutile, is commonly used as the basic colouring component, subsequently being tinted with other pigments to offer a range of colour shades.

This paper describes the substitution of rutile TiO_2 with the alternate TiO_2 crystalline form of anatase, that being photocatalytic in a nano-particle size. Two series of samples were suggested and produced, the first set was retained at common conditions (reference specimens) whereas the second series of samples was exposed to UV radiation. Then, differences between the main physical and mechanical properties of the two series were examined.

Key words: *paste, facade, render, photocatalysis, titanium dioxide, adhesive strength, water vapour permeability, water resistance*

1. INTRODUCTION

Surface treatments of engineering constructions are nowadays a relatively important part of buildings, simultaneously improving their aesthetic appearance and not least their durability. Established lime or cement-based plasters have almost disappeared from surface treatment materials. At present manufactured complete facade renders in paste form intended for final exterior surface adjustment are preferred.

Now, in connection with nanotechnology development, new properties may be assigned to facade renders. Particularly it is necessary to mention the photocatalytic activity of the plaster surface, offering an ability to break down contaminants from the facade surface. The influence of photocatalysis on basic physical and mechanical properties is described in this article.

2. PHOTOCATALYSIS

Titanium white nano-elements in anatase crystalline diversification show photocatalytic parameters. Due to this ability it is possible to reduce undesirable chemical compounds. For example, the decomposition of organic and inorganic pollutants in addition to micro-organisms, which is an

important consideration in context of this fact [2]. The aforementioned process is known as photocatalytic oxidation.

The principle of such a system is that of a semiconductor, whereat photon absorption and then electron transition (from non-conducting to conducting zone) occurs following irradiation with light of a suitable wave length (UVA). The process is called the photogeneration coupling of an electron-hollow [1]. Then the electrically positive hollow reacts with a water molecule (e.g. from air humidity) creating a hydroxylic radical and a proton. Afterwards the second pair electron reacts with a oxygen molecule and proton. Result of the second reaction is a peroxo-radical (see below scheme).

$$d^+ + H_2O \rightarrow {}^{\bullet}OH + H^+ \qquad (1)$$

$$e^- + O_2 + H^+ \rightarrow {}^{\bullet}OOH \qquad (2)$$

The aforementioned two reactions are the first step of photocatalysis. The next reactions lead to single organic compound decomposition. This confirms a choice suitability of silica-metal based paste plasters, which show a minimal amount of organic compounds and therefore that significant degradation is not taking place.

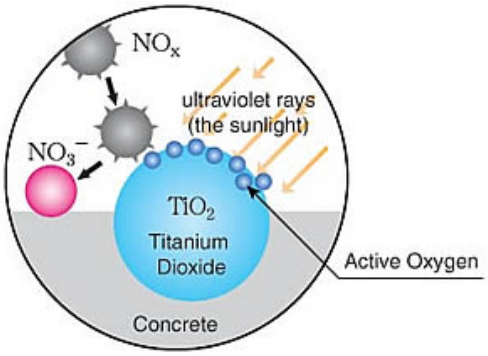


Figure 1. Photocatalysis principle [2]

The hydroxylic radical pulls up a hydrogen atom from an organic molecule, thereby an organic radical and water are created. Thereinafter the created organic radical reacts with the oxygen molecule and thereby an organic peroxo-radical is formed. Overall, two oxygen molecules are made more active due to the energy of a photon. Consequently, reaction between the hydroxyl radical and the organic peroxo radical is imminent producing unstable organohydrotetraoxide, which is continuously disintegrating. Ideally degradation to carbon oxide and water is occurring [2]. The basic principle of a photocatalytic reaction is shown in the Figure 1.

3. SAMPLE PREPARATION

Testing follows from the checking of organic compound degradation in the plasters after UVA irradiation exposure. For the purpose of improving workability in the fresh state and increasing the mature plasters' elasto-plastic parameters, an organic compounds content was incorporated into silicate plaster samples (up to weight 15%). These substances surround the pigment particles and thereby suppress their photocatalysis activity, at least in the first instance, until they reach their mastication.

On this account it was necessary to verify how the UV irradiation effects work upon the chosen and most commonly monitored parameters of silicate paste renders. In connection with the above mentioned, basic physical and mechanical properties were investigated at The Technology of Building Materials and Components Institute (Brno University of Technology, Faculty of Civil Engineering):

- determination of water vapour permeability,
- determination of adhesive strength,
- determination of water resistance,
- determination of frost resistance,
- determination of temperature variations (sudden temperature change resistance).

Silicate plaster samples with limestone aggregate and other additives including 4% TiO_2 (in a various forms) were prepared for the purposes of testing according to aforementioned methods (see Table 1).

Table 1 – Characteristic of single specimen batches

Batch	Plaster type	TiO_2 used type
1	Silicate paste render (max. particle size 1,5mm)	Chloride rutile **4% CR-826, Tronox partical size circa 200nm**
2	Silicate paste render (max. particle size 1,5mm)	Anatase **4% AV-01 SF, Precheza partical size circa 180nm**
3	Silicate paste render (max. particle size 1,5mm)	Nano-Anatase **4% FA-60, Precheza partical size circa 60nm**

All testing samples of plasters were applied to screeding slabs except for the specimens destined for water vapour permeability determination, which were appiled to filter paper.

Quantity and composition of the samples is evident from the result tables. For research purposes approximately 90 samples were produced, whereas half of the samples were exposed UV radiation (QUV panel with parameters of intensity 0,55 $W.m^{-2}$, and wave length 340 nm was used) for 756 hours. The second half were retained at normal laboratory conditions (dark and dry room). It is necessary to mention that three different batches were proposed (see Table 1).

4. EXPERIMENTAL STUDY

4.1 Water vapour permeability determination

The determination of water vapour permeability was performed according to standard ČSN EN 1015-19. Testing samples (applied on filter paper) were fixed to an open circular dish by a suitable binder (silicone). It was necessary to maintain constant water vapour pressure surrounding the dishes by means of saturated salt solutions. In our case a KNO_3 solution was used, which ensured relative air humidity of 93.2 % with a temperature of 20 degrees Celsius. The dishes with the samples were stored in a conditioning chamber, making it possible to maintain constant values of water vapour pressure and temperature. With regard to fact that a upper hygroscopicity range was chosen, climatic conditions of relative humidity 50 (±5) % and temperature 20 (±2)°C were required to be established in the conditioning chamber. The principle consisted of weight loss logging and determination over suitable time periods. The weight of the samples was monitored and noted until constant climatic conditions in the dishes were accrued, i.e. three successive weight losses were coincident independent of time. Then water vapour penetration was determined from the measured values according to the formula:

$$\Lambda = \frac{1}{A\Delta_p / (\Delta G / \Delta t) - R_A} \left[kg / m^2 .s.Pa \right]$$

where:

A area of open circular dish in m^2,

Δ_p difference of salt solution water vapour pressure and surrounding climatic pressure is read from appropriate tables in Pa,

$\Delta G/\Delta t$ water vapour flow in kg/s,

Λ water vapour penetration in $kg/m^2.s.Pa$,

R_A air layer water vapour resistance between test specimen and salt solution in $Pa.m^2.s/kg$ (for air layer of 10 mm is $0{,}048 \times 10^9$ $Pa.m^2.s/kg$)

Table 1 – Water vapour permeability measured and computed data

Batch	Specimen	$\Delta G/\Delta t \times 10^9$ [$kg.s^{-1}$]	$\Lambda \times 10^9$ [$kg/m^2.s.Pa$]	$d \times 10^3$ [m]	Permeability$\times 10^{12}$ [$kg.m^{-1}.s^{-1}.Pa^{-1}$]	Average $\times 10^{12}$ [$kg.m^{-1}.s^{-1}.Pa^{-1}$]
1	11	-10,8	1,98	2,81	5,60	**4,78**
	12	-7,89	1,43	3,00	4,30	
	13	-8,04	1,46	3,05	4,50	
	11ir	-11,60	2,14	2,78	5,90	**5,04**
	12ir	-8,27	1,51	3,00	4,50	
	13ir	-8,51	1,55	3,00	4,70	
2	21	-8,04	1,46	2,85	4,20	**5,20**
	22	-10,3	1,89	3,18	6,00	

Batch	Specimen	$\Delta G/\Delta t \times 10^9$ [kg.s^{-1}]	$\Lambda \times 10^9$ [kg/m^2.s.Pa]	$d \times 10^3$ [m]	Permeability$\times 10^{12}$ [kg.m^{-1}.s^{-1}.Pa^{-1}]	Average $\times 10^{12}$ [kg.m^{-1}.s^{-1}.Pa^{-1}]
	23	-9,61	1,76	3,09	5,40	
	21ir	-8,33	1,52	2,83	4,30	
	22ir	-10,80	1,98	3,18	6,30	**5,46**
	23ir	-10,30	1,89	3,06	5,80	
	31	-10,9	2,00	3,10	6,20	
	32	-12,1	2,23	2,88	6,40	**5,76**
	33	-8,78	1,60	2,91	4,70	
3	31ir	-11,80	2,17	3,05	6,60	
	32ir	-13,00	2,39	2,88	6,90	**6,13**
	33ir	-9,32	1,70	2,88	4,90	

N.B. Symbol *d* expresses sample thickness in Table 1. Symbol *ir* indicates the samples were irradiated.

4.2 Adhesive strength determination

Adhesive strength determination was carried out according to ČSN EN 1015–12. Iron discs of 50 mm diameter were used for the testing. Two component epoxy resin based adhesive was applied for the fixation of the discs. Following the curing of the adhesive the iron discs were trimmed about the edge to an octagon shape so that sections intervened in screeding of samples. Thereby the load area was exactly defined. For adhesive strength determination a device called DYNA Z 15 was used. The strength was calculated in compliance with formula:

$$f_u = \frac{F_u}{A}\left[N/mm^2\right]$$

where f_u is adhesive strength in v N/mm^2,

F_u is ultimate breaking load in N,

A is circle test area in mm^2 (cca 1962,5 mm^2).

Table 2 – Adhesive strength determination results

Batch	Specimen	F_u [kN]	Failure mode	f_u [N.mm^{-2}]	Ø f_u [N.mm^{-2}]
	11	1,02	b[2]	0,52	
1	12	1,08	b	0,55	**0,54**
	13	1,09	b	0,56	

[2] Possible failure modes are shown in Figure 1.

Batch	Specimen	F_u [kN]	Failure mode	f_u [N.mm^{-2}]	Ø f_u [N.mm^{-2}]
	11ir	1,47	b	0,75	
	12ir	1,43	b	0,73	**0,73**
	13ir	1,40	b	0,71	
2	21	0,94	b	0,48	
	22	0,88	b	0,45	**0,48**
	23	0,99	b	0,50	
	21ir	1,13	b	0,58	
	22ir	1,31	b	0,67	**0,63**
	23ir	1,26	b	0,64	
3	31	1,09	b	0,56	
	32	0,92	b	0,47	**0,50**
	33	0,92	b	0,47	
	31ir	1,19	b	0,61	
	32ir	0,87	b	0,44	**0,52**
	33ir	1,01	b	0,51	

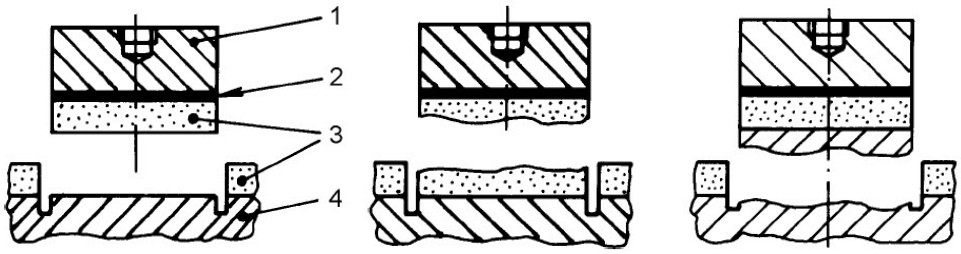


Figure 1.Possible failure modes ;left – type a – grip failure, results are examination of adhesive strength; middle – type b – cohesion failure, adhesive strength is over than achieved test result; right – type c – cohesion failure, adhesive strength is over than achieved test result); 1 – test circle, 2 – adhesive layer, 3 – mortar (surface treatment), 4 - bedding.

4.3 Water resistance determination

Water resistance determination was performed in step with the standard s ČSN 72 2578. The principles of the test involve the measuring of an amount of water which saturates the specimen during a fixed term. Surface treatment water resistance V_{30} in l.m^{-2} was then determined according to formula:

$$V_{30} = \frac{\Delta l}{A}$$

where Δl is water loss in litres per 30 minutes,

A is doused area in m^2.

The test result is the arithmetic mean of the two minimally measured values. The outcome is accurate if the determined values are lower than or equal to the project prescribed value or appropriate technical specification. Nevertheless the water resistance of outdoor surface treatments may produce higher values such as 2 $l.m^{-2}$ per 30 minutes.

Table 3 – Water resistance determination results

Batch	Specimen	Δl [l]	V_{30} [$l.m^{-2}$]	Ø V_{30} [$l.m^{-2}$]
1	11	0,0025	0,9	**0,9**
	12	0,0026	0,9	
	13	0,0023	0,8	
	11ir	0,0025	0,9	**0,8**
	12ir	0,0023	0,8	
	13ir	0,0021	0,7	
2	21	0,0021	0,7	**0,9**
	22	0,0025	0,9	
	23	0,0028	1,0	
	21ir	0,0015	0,5	**0,7**
	22ir	0,0025	0,9	
	23ir	0,0020	0,7	
3	31	0,0007	0,2	**0,3**
	32	0,0006	0,2	
	33	0,0009	0,3	
	31ir	0,0004	0,1	**0,2**
	32ir	0,0008	0,3	
	33ir	0,0005	0,2	

4.4 Frost resistance determination

Frost resistance determination was performed according to standard ČSN 73 2579. The principle of this method being the exposure of the surface of the test specimen to alternating freezing and thawing to a number of nominated freezing cycles (minimum of 15 cycles). In this case the effect of 50 freezing cycles was investigated. Following cycle completion an assessment of adhesive strength was undertaken. Generally is has been true that a surface treatment complies with frost resistance if adhesive strength values are at least 0,25 N/mm^2 after 15 freezing cycles (for synthetic plaster). The results appear to comply with this whilest subgrade material failure was achieved with values lower than 0,25 N/mm^2 .

Table 4 – Result of frost resistance determination after 50 cycles

Batch	Specimen	F_u [kN]	Failure mode	f_u [N.mm^{-2}]	Ø f_u [N.mm^{-2}]
1	11	0,47	b	0,24	**0,25**
	12	0,47	b	0,24	
	13	0,51	b	0,26	
	11ir	1,18	b	0,60	**0,58**
	12ir	1,27	b	0,65	
	13ir	0,99	b	0,50	
2	21	0,53	b	0,27	**0,30**
	22	0,60	b	0,31	
	23	0,61	b	0,31	
	21ir	1,41	b	0,72	**0,60**
	22ir	1,17	b	0,60	
	23ir	0,94	b	0,48	
3	31	0,67	b	0,34	**0,31**
	32	0,66	b	0,34	
	33	0,49	b	0,25	
	31ir	1,25	b	0,64	**0,61**
	32ir	1,21	b	0,62	
	33ir	1,13	b	0,58	

4.5 Sudden temperature changes resistance determination

The test for the resistance of the surface finish of building structures to temperature variation was carried out in accordance to standard ČSN 73 2581. The principle of the test is similar to the previously described method. The warming of the surface treatment was performed with the aid of infra heaters at a temperature of 70(±3)°C (per 30 - 40 minutes) and subsequently a water sprinkler was used for cooling to a temperature of 20(±2)°C (per 5 - 10 minutes) in 25 test cycles. Determination of adhesive strength then followed. Visual checking, detection of the creation of pertinent cracks and sample failure (bubbles, peeling etc.) was performed after each temperature cycle. Surface treatment (for synthetic plaster) complies with temperature variations if the adhesive strength values are at least 0.25 N/mm^2 after 25 cycles. The results generally comply with this whilst material failure on values lower than 0,25 N/mm^2 is achieved.

Table 5 – Sudden temperature changes resistance results after 25 cycles

Batch	Specimen	F_u [kN]	Failure mode	f_u [N.mm^{-2}]	Ø f_u [N.mm^{-2}]
1	11	0,64	a	0,33	**0,25**
	12	0,48	a	0,24	
	13	0,34	a	0,17	
	11ir	0,73	b	0,37	**0,51**
	12ir	1,18	b	0,60	
	13ir	1,09	b	0,56	
2	21	1,17	b	0,60	**0,35**
	22	0,18	a	0,09	
	23	0,73	a	0,37	
	21ir	2,17	a	1,11	**1,13**
	22ir	2,32	b	1,18	
	23ir	2,19	b	1,12	
3	31	1,15	a	0,59	**0,83**
	32	1,83	a	0,93	
	33	1,88	b	0,96	
	31ir	2,30	b	1,17	**1,19**
	32ir	2,66	a	1,35	
	33ir	2,04	b	1,04	

5. RESULTS AND DISCUSSION

The evaluation of physical and mechanical characteristics of the investigated TiO_2 based renders is illustrated in graphic form by the following, (Figures 3-7). It is clearly evident that the performance of the different batches and irradiated samples is related to their composition, this being a positive affirmation of this research. Tables and graphs show conclusively that the best water vapour permeability is evident in the irradiated surface treatment specimens of batch no. 3 (see Figure 3). This is caused by the render surface opening due to the degradation of organic compounds owing to the UV effect on Anatase TiO_2 nano-particles. Also apparently this is related to TiO_2 particles size (see Table 1). The water vapour permeability is significant in connection with the free flight of humidity from the masonry of building structures, where undesirable material degradation could occur. In some ways a no less substantial parameter which determines the technological properties of renders (for surface treatment of building exteriors) is fixation on bedding, which was proved by adhesive strength determination (see Figure 4).

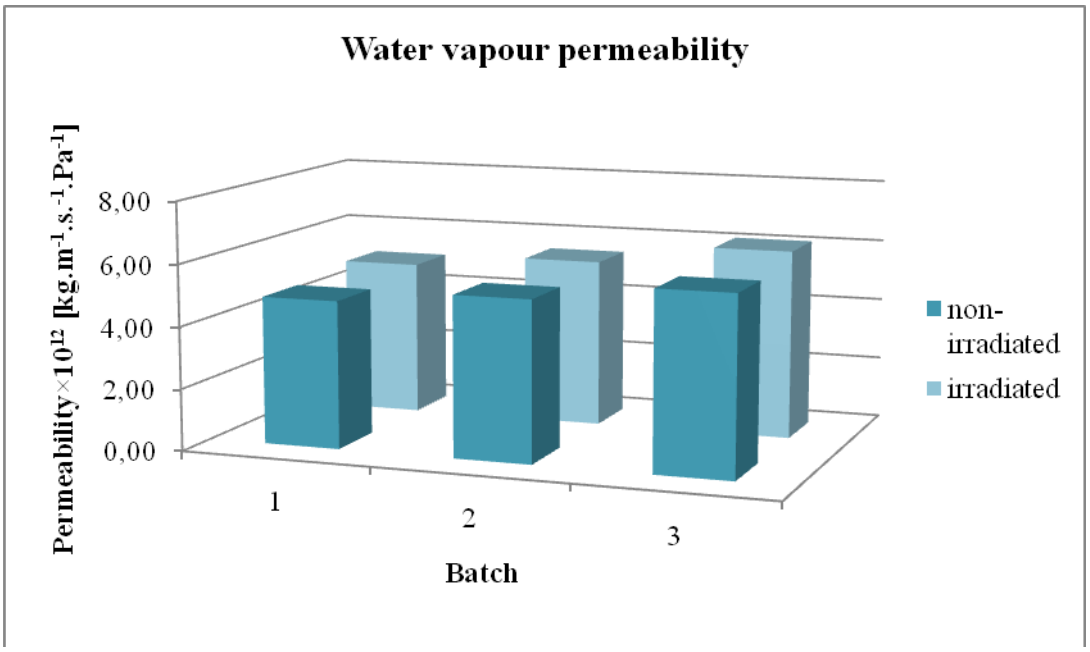


Figure 1. Water Vapour Permeability: Comparison of medial values of individual batch samples.

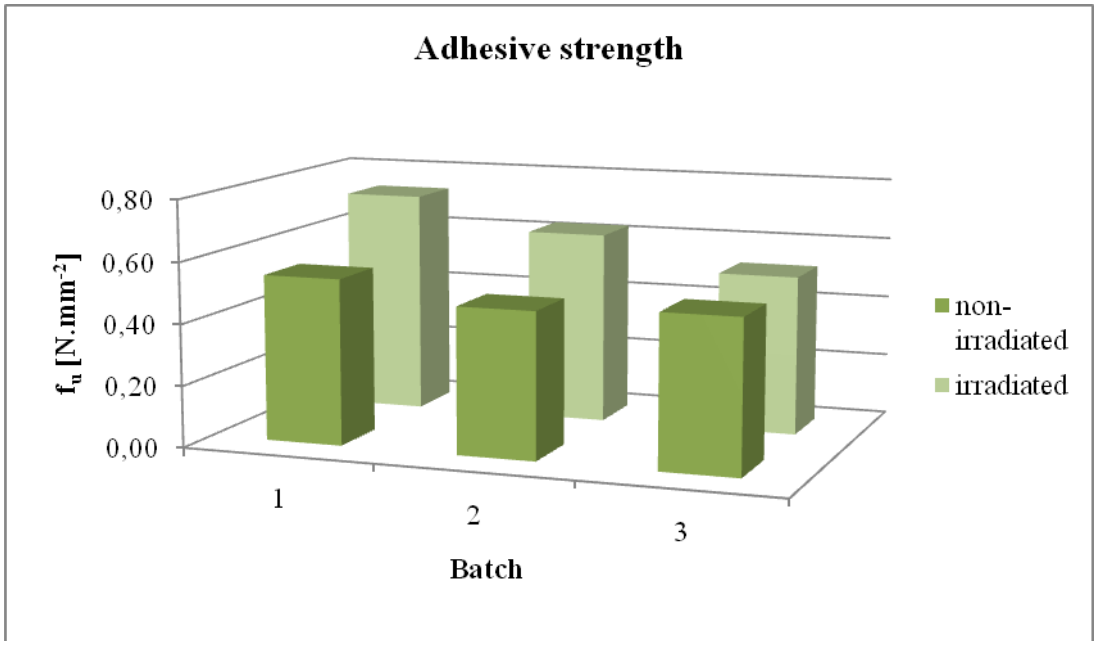


Figure 2. Adhesive Strength: Comparison of medial values of individual batch samples.

The graph in figure 2 illustrates conclusively that the best fixation ability appeared in irradiated samples prepared from batch no. 1, where organic compounds are not degraded by photocatalysators. Further more, it is apparent that the irradiated specimens performed much better than non-irradiated samples, which is due to a 28 days maturing period.

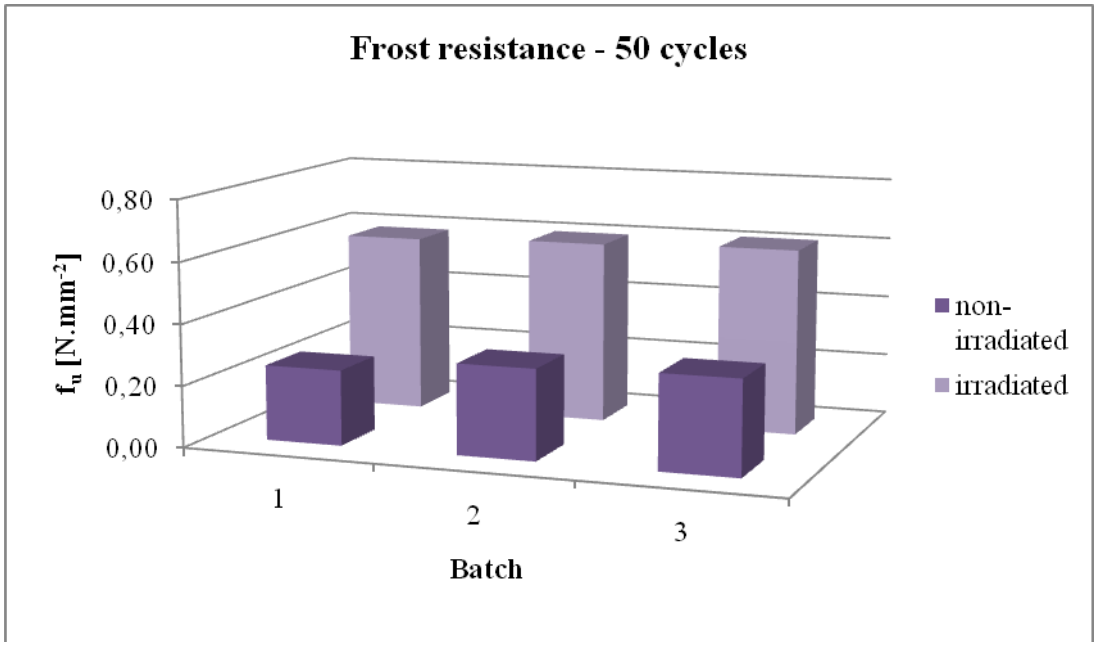


Figure 3. Frost Resistance: Comparison of medial values of individual batch samples.

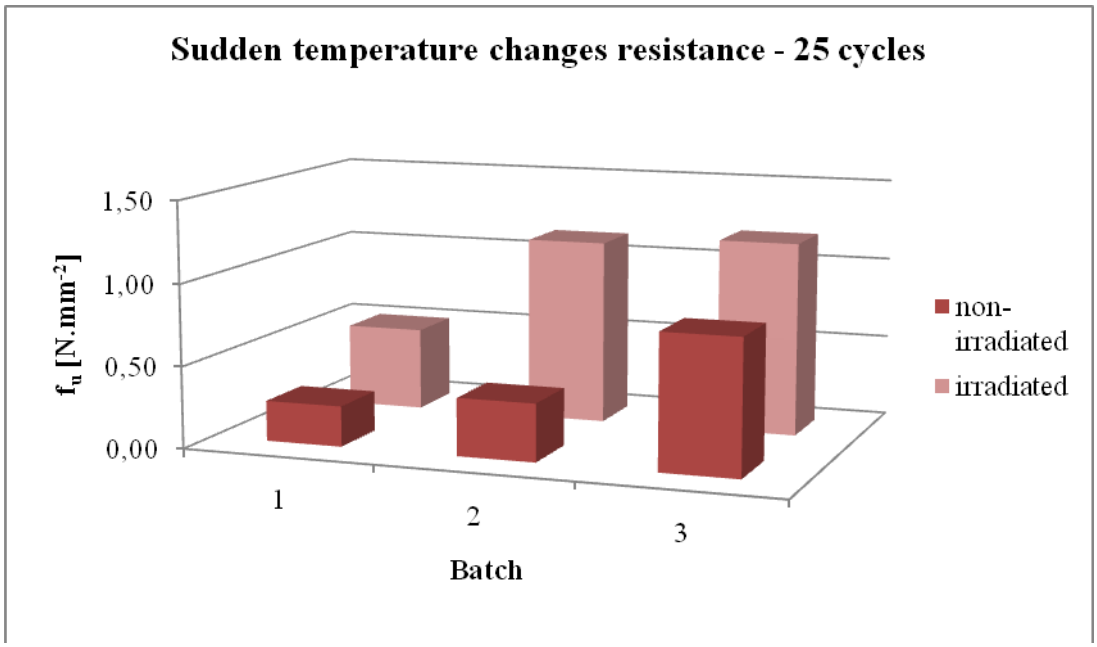


Figure 4. Sudden Temperature Change Resistance:
Comparison of medial values of individual batch samples.

In the case of frost and sudden temperature change resistance, the effect of radiation exposure was significantly more evident than in the adhesive strength investigation. Graphs in Figures 2, 3 and 4 clearly illustrate this fact, whereas using batch no. 3 (with photocatalysators) appears optimal in comparison to the others. All of the specimens (irradiated and non-irradiated) meet standard requirements for adhesive strength, i.e. $f_u \geq 0{,}25$ N.mm^{-2}.

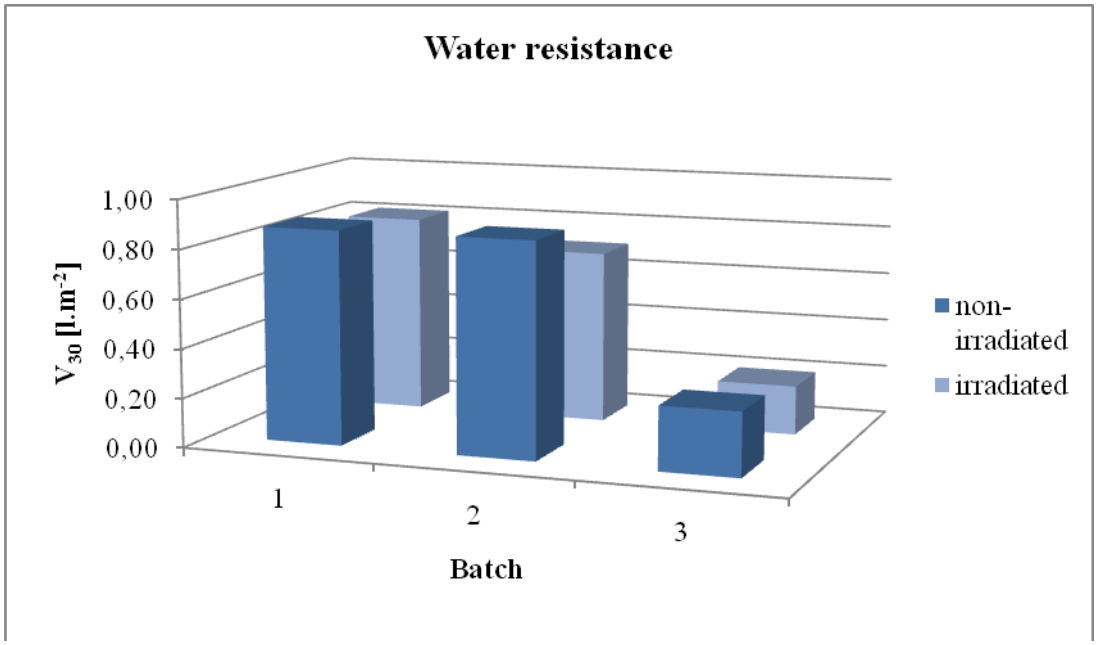


Figure 5. Water Resistance: Comparison of medial values of individual batch samples.

In terms of surface treatment application on buildings facing exterior climatic conditions, water-resistance of facade renders can be considered as a lesser significant criterion. In Figure 5 the better parameters of irradiated samples are apparent once again together with the excellent water resistance of batch no. 3 specimens being evident. Standard requirement of $V_{30} \leq 2$ l.m^{-2} was achieved in the case of all samples (irradiated and non-irradiated).

6. CONCLUSIONS

By virtue of tests undertaken and results achieved it can be stated that all of the facade render samples met the minimum standard demands for their determined properties, i.e. frost resistance, sudden temperature change resistance and water resistance. From data evaluation it is evident that UV irradiated samples show better properties than non-irradiated samples, throughout most of the tests and determination.

The research proved that organic additives, which are put into plasters for purpose of parameter modification have an effect only in the fresh render state at the time of application, subsequently certain properties may be even worse. Renders containing photocatalytic TiO_2 nano-particles demonstrated not only their utility in this case, leading up to plaster which has an opened porous structure with the degradation of organic additives, but additionally these renders are able to clean organic pollutants from their surface layer, which reduces maintenance.

ACKNOWLEDGEMENTS

This paper was published with the financial contribution of research project CEZ - MSM 0021630511, "Progressive Building Materials with Utilization of Secondary Raw Materials and their Impact on Structure Durability".

REFERENCES

1. KELLER, A. Chemistry and Applications of Photocatalytic Oxidation of Thin Organic Films, Acc. Chem. Res. 1995,28, 503-508.

2. EINAGA, H.; FUTAMURA, S.; IBUSUKI, T. Photocatalytic decomposition of benzene over TiO_2 in a humidified airstream, Phys. Chem. Chem. Phys., 1999, 1, 4903-4908.

4. ČSN EN 1015-19 Methods of test for mortar for masonry – Part 19: Determination of water vapour permeability of hardened rendering and plastering mortars

5. ČSN EN 1015–12 Methods of test for mortar for masonry – Part 12: Determination of adhesive strength of hardened rendering and plastering mortars on substrates

6. ČSN 72 2578 Test for water resistance of the surface finish of building structures

7. ČSN 73 2579 Test for frost resistance of the surface finish of building structures

8. ČSN 73 2581 Test for resistance of the surface finish of building structures to temperature variations